Polymer Degradation and Stability 191 (2021) 109672

Contents lists available at ScienceDirect

Polymer Degradation and Stability

journal homepage: www.elsevier.com/locate/polymdegradstab

Pyrolysis mechanism of phenylboronic acid modified phenolic resin

Xiaolong Xing[a,1], Ping Zhang[a,1], Yuhong Zhao[a], Fei Ma[c], Xiaoting Zhang[a], Fang Xue[a], Shujuan Wang[a], Xinli Jing[a,b,*]

[a] School of Chemistry, Xi'an Jiaotong University, Xi'an, Shaanxi, 710049, People's Republic of China
[b] Xi'an Key Laboratory of Sustainable Energy Material Chemistry, Xi'an, Shaanxi, 710049, People's Republic of China
[c] Xi'an Aerospace Composites Research Institute, Xi'an, Shaanxi, 710025, People's Republic of China

ARTICLE INFO

Article history:
Received 2 April 2021
Revised 6 July 2021
Accepted 11 July 2021
Available online 15 July 2021

Keywords:
Phenolic resin
Phenylboronic acid
Pyrolysis mechanism
Volatile organic compounds
Char yield

ABSTRACT

Phenylboronic acid (PBA) modified phenolic resin (PBPR) is one of the most important phenolic resins (PR) due to its good processability and high char yield. However, the pyrolysis mechanisms of PR and PBPR still remain poorly understood, which imposes limits on the synthesis, development and application of these materials. In this work, the pyrolysis process of PBPR has been studied through novolac resin (NR) and PBA crosslinked NR (PBNR) at high temperatures, and the reasons for the high char yield of PBPR were explored, as well. According to the results, the pyrolysis of NR begins with the cleavage reaction of the covalent single bonds in the molecular backbone. The release of volatile organic compounds (VOCs) such as monophenols and bisphenols formed by the cleavage of C—C single bonds is the major cause of the decreased char yield of NR at elevated temperatures. Meanwhile, increasing NR molecular weight and crosslinking NR could reduce the formation probability of VOCs, which is beneficial to obtaining the high char yield resin. In PBPR, the boronic ester linkages make the formation of VOCs more difficult and contribute to the high char yield of resin. The present work provides guiding significance for deeply understanding the pyrolysis mechanism of PR and PBPR to ensure their high thermal stability and char yield at high temperatures.

© 2021 Elsevier Ltd. All rights reserved.

1. Introduction

Being one of the most important thermosetting resins, phenolic resin (PR) is widely used in advanced composite materials. PR is especially commonly applied as the matrix resin for ablation-resistant composites or precursors for C/C composites for thermal protection systems due to its good processability and high char yield [1]. However, the rapid development of related technologies in the aerospace field has put forward stringent demands for ablation-resistant materials [2]. To effectively improve the ablative performance of PR, it is crucial to understand the detailed mechanism during the pyrolysis process. According to the reported studies on the pyrolysis process of PR [3–5], two representative pyrolysis mechanisms have been proposed. One is the three-stage pyrolysis mechanism of PR, which can be described by a sequence of the following steps [6]. First, the additional crosslinking points arise due to the condensation reactions between the functional groups of the cured PR. Second, some crosslinking points of cured PR are broken, leading to the evolution of methane, hydrogen, and carbon monoxide. Third, dehydrogenation of benzene leads to the release of hydrogen. Another mechanism proposed by Jackson et al. [7] implies that pyrolysis of PR is an oxidative degradation process even though occurring in an inert environment, and the pyrolysis products provide the source of oxygen. Regardless of relative completeness, both the theories contradict each other on whether carbonyl and hydrogen form during pyrolysis.

Various attempts have been made to modify the PR to improve its thermal stability, such as introducing boron (B) [8–10], phosphorus (P) [11,12], silicon (Si) [13–15], or other chemical elements. Among them, the boric acid modified PR (BPR) is one of the most important products due to its good thermal stability, especially high thermal decomposition temperature and elevated char yield [16]. BPR was first reported by Sporzynski et al. [17] in 1951, the thermal decomposition temperature at 10% weight loss ($T_{10\%}$) of resin from 285 to 345 °C and achieve 71% of the char yield at 800 °C ($R_{800°C}$) in nitrogen atmosphere [18]. However, the application of BPR is still greatly limited because of its poor processability and mechanical property. Even though the structure and properties of BPR have been thoroughly described [19,20], the underlying reasons for its excellent thermal stability have not yet been fully explained. Based on the study of hyperbranched polyborate and its

* Corresponding author.
E-mail addresses: xljing@mail.xjtu.edu.cn, rgfp-jing@mail.xjtu.edu.cn (X. Jing).
[1] These authors contributed equally to this work.

https://doi.org/10.1016/j.polymdegradstab.2021.109672
0141-3910/© 2021 Elsevier Ltd. All rights reserved.

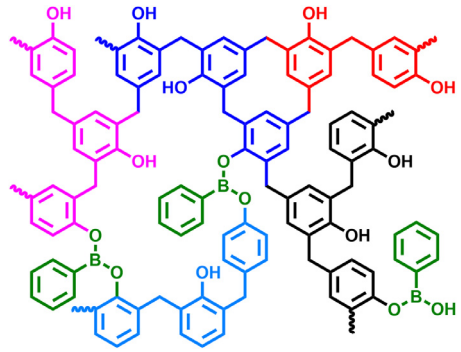

Fig. 1. The possible crosslinking structure of PBPR.

modified PR [21–23], we developed the phenylboronic acid (PBA) modified PR (PBPR) [24,25] with the processability similar to that of PR, whereas its thermal stability and mechanical properties of the composite material were far superior to those of BPR. These are due to the specific crosslinking structure of PBPR (see in **Fig. 1**), making it a more promising ablative resin. The amount of boronic ester linkages in PBPR is not enough to form the three-dimensional crosslinking network, so the crosslinking structure of PBPR is still formed by methylene-linked phenols, and boronic ester only blocks the phenolic hydroxyl group. Therefore, the crosslinking structure of PBPR can be regarded as the boronic ester linkages formed in the cured PR.

Although the various opinions that have been put forward could be used to understand the excellent thermal stability of BPR, the pyrolysis mechanisms of PR and PBPR remain poorly understood. Up to now, four essential viewpoints have been proposed to elucidate the reason for the high char yield of PBPR. Firstly, the high char yield of PBPR is due to the high bond dissociation energy of B—O bond (774 kJ/mol) [26]. However, the high bond dissociation energy of the B—O bond cannot influence the bonding strengths of nearby covalent bonds in the PBPR crosslinking network, such as the C—H and C—C bonds of methylene and the O—H of phenol. Secondly, the activity of the phenolic hydroxyl groups will be reduced due to the esterification of the boron hydroxyl groups [27,28]. Because phenolic hydroxyl groups are the active sites of thermal instability in PR, and the formation of boronic ester linkages in PBPR restrains their reaction. It is noteworthy that many phenol hydroxyl groups are still present in PBPR. Thirdly, the formation of the boron oxides during pyrolysis is situated on the carbonized surface of the product and prevented the oxidation process [29,30]. In addition, the boron oxides at high temperatures reduce the number of small molecules of carbon oxides, which is conducive to the improvement of the PBPR's char yield. Actually, this viewpoint is suitable for describing the pyrolysis in an oxygen atmosphere rather than the pyrolysis in an inert medium. Fourthly, the boronic ester linkages change the pyrolysis mechanism of PR and contribute to the carbonization of PR [25]. Since the boronic ester linkages in PBPR bring more adjacent benzene groups, this is likely the key reason for the high char yield of the cured PBPR during the high temperature pyrolysis. Although the fourth viewpoint is considered more relevant to the actual situation, the research cannot illustrate the actual pyrolysis process of PBPR. The elucidation of the pyrolysis mechanism of PBPR based on PR's pyrolysis details is the main goal of this paper based on the pyrolysis mechanism of PR.

The current research on the pyrolysis mechanism of PR mainly focuses on the cured resin. However, the limited understanding of the structural characteristics of cured resin leads to the lack of information about its pyrolysis mechanism. Meanwhile, the crosslinking structure of PBPR can be regarded as the boronic ester linkages formed in the cured PR. We have preliminarily clarified the early pyrolysis process of novolac resin (NR) through ReaxFF-molecular dynamics (ReaxFF-MD) simulation [31]. This study aims to explain the high char yield of PBPR based on the further understanding of the pyrolysis process of NR and PBA crosslinked NR (PBNR) via the thermogravimetric (TG) analysis and the pyrolysis-gas chromatography/mass spectrometry (Py-GC/MS) technique. First of all, we realized that the weight loss during the pyrolysis process of NR is mainly caused by the release of volatile organic compounds (VOCs) such as monophenols and bisphenols. The influence of molecular weight and crosslinking on the pyrolysis process of NR has been investigated. Furthermore, the effect of introduced boronic ester linkages on the pyrolysis process of NR was assessed. It is essential to mention that we agree with peers in the understanding of the crosslinking structure and pyrolysis products of PR [32,33], and there is no relevant structural characterization carried out in this study. The main focus of the present work is on providing a new understanding of the pyrolysis process of NR and pointing out for the first time that the volatilization of VOCs produced by methylene cleavage is the root cause of the reduced char yield of PR. Therefore, the study is of great value for developing PR with high thermal stability and promoting its wide application in ablation-resistant composites and related fields.

2. Experimental

2.1. Materials

Acetone, petroleum ether with a boiling range of 60 - 90 °C, hexamethylenetetramine (HMTA), and ethanol were supplied by Sinopharm Chemical Reagent Co., LTD. PBA with a purity of great than 99.0% and purchased from TCI America. The NR (NR-8063-2) was supplied by Shandong Shengquan Chemical Co., LTD, denoted as NR0. The free phenol content in NR0 is less than 0.50%, the softening point of NR0 is about 115 - 120 °C, the hydroxyl equivalent is 107 - 110 g/eq, the sodium ion content is less than 5 ppm, and the chlorine ion content is less than 4 ppm. All materials were used as received without further purification.

2.2. Preparation of the HMTA crosslinked NR

The NR0/HMTA mixtures were obtained through the solution method with ethanol as the solvent. NR0 and HMTA were dissolved in ethanol to prepare a 60 wt.% solution. The solution was concentrated using the rotary evaporator and dried at room temperature in the vacuum oven to obtain the NR0/HMTA mixture. The NR0/HMTA mixture was weighed every 0.5 h until the weight was constant, and then the sample was ground into the fine powder (about 80 mesh). The powder was placed in the polytetrafluoroethylene (PTEF) vessel and cured at 170 °C for 2 h under nitrogen protection. The NR0 cured with 4, 8, 12, and 16 parts per hundreds of resins (phr) of HMTA were named as HNR-4, HNR-8, HNR-12, and HNR-16, respectively.

2.3. Preparation of PBNR

The NR0/PBA mixtures with different PBA dosages were prepared by solution blending. NR0 and PBA were dissolved in acetone at room temperature and stirred by the magnetic stirrer for about 5 h to obtain a homogeneous solution. The solution was concentrated using the rotary evaporator and dried at room temperature in the vacuum oven to get the NR0/PBA mixture. The NR0/PBA mixture was weighed every 0.5 h until the weight was constant, and then the sample was ground into the fine powder (about 80 mesh). The powder was placed in the PTEF vessel and continuously cured under nitrogen protection through the isothermal process of

160 °C at 2 h and then 180 °C at 4 h [34]. We have used XPS, FTIR, solid-state ^{13}C NMR and ^{11}B NMR technologies to determine that PBA has been incorporated into the PBNR structure, and the B—O—C and B—O—B linkages have been formed in crosslinking network. The cured PBNR samples using 5, 10, 20, 30, 40, 60 and 80 phr of PBA were named PBNR-5, PBNR-10, PBNR-20, PBNR-30, PBNR-40, PBNR-60 and PBNR-80, respectively.

2.4. Characterization

The Gel Permeation Chromatography (GPC) measurements were performed using Agilent PL-GPC50 (Agilent, USA) consisting of PL-gel MIXED-D gel column (300 mm × 7.5 mm, 5 μm) and refractive index detector with the flow rate of 1.0 mL/min at 40 °C, and tetrahydrofuran was used as the carrier solvent. A linear calibration curve with polystyrene standards was made to determine the molecular weight and polydispersity of the resin.

The Py-GC/MS analyses were performed using Frontier PY-2020S tubular furnace cracker. The sample injection quantity was 0.5 g and the pyrolysis temperatures were 200, 300, 400, 500 and 600 °C, respectively. The pyrolysis gas was helium with the flow rate of 3 mL/min. The sample was injected at 40 °C, and then heated up to 260 °C at the heating rate of 5 °C/min after holding for 3 min, and kept at 260 °C for 10 min. The gas was analyzed by GC/MS-QP2010 (Shimadzu, Japan), and the volatilizations with m/z values between 25 and 400 au were taken as the Py-GC/MS analysis results.

The TG analyses were carried out using the NETZSCH TG 209C (NETZSCH, Germany), and the sample was heated from 30 to 800 °C at the heating rate of 10 °C/min under the nitrogen atmosphere with the flow rate of 50 mL/min.

The differential scanning calorimetry (DSC) analyses were performed on the NETZSCH DSC 200PC (NETZSCH, Germany) under nitrogen atmosphere at the heating rate of 10 °C/min from 30 to 300 °C with an empty aluminum pan as the reference. The test process to determine the glass transition temperature needs to eliminate the thermal history of the samples. Specifically, the temperature was increased from 30 to 120 °C at the heating rate of 20 °C/min, and then the temperature was reduced to 0 °C with the cooling rate of 20 °C/min.

The TGA-GC/MS-FTIR analyses were performed on the PerkinElmer TL 9000e (PerkinElmer, USA) under helium atmosphere at the heating rate of 10 °C/min from 30 to 800 °C. The sample was injected in GC/MS at 40 °C, and then heated up to 260 °C at the heating rate of 5 °C/min after holding for 3 min, and kept at 260 °C for 10 minutes. The resolution of FTIR is 8 cm^{-1}.

3. Results and discussion

3.1. The pyrolysis mechanism of NR

3.1.1. Homolytic reaction and formation of VOCs during the pyrolysis of NR

The pyrolysis process of polymer begins with the cleavage reaction of covalent bonds during heating to a high temperature [35], especially the covalent single bonds with lower bond dissociation energy are broken first. Based on the understanding of the NR pyrolysis process through ReaxFF-MD simulation [31], the pyrolysis of NR can be divided into the cleavage reactions on the backbone (CR_o, referring to the C—C single bonds) and the ones beside the backbone (CR_b, including C—H, O—H, and C—O single bonds), as shown in **Scheme 1**. The phenolic compounds are mainly formed by the CR_o process, among them the release of monophenol and bisphenol compounds results in weight loss, which is the focus of this study. The H_2O and permanent gases are formed by the CR_b, among which H_2O and H_2 are the earliest molecules in the system.

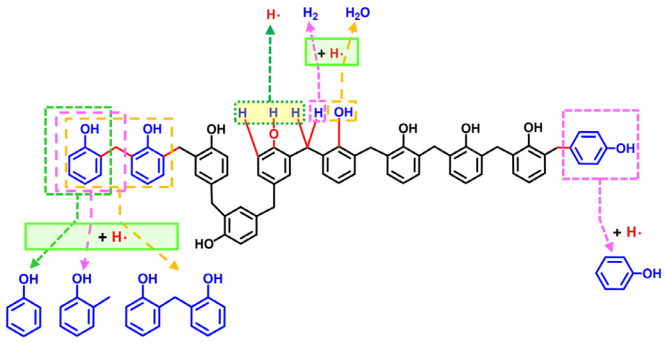

Scheme 1. The pyrolysis process of NR.

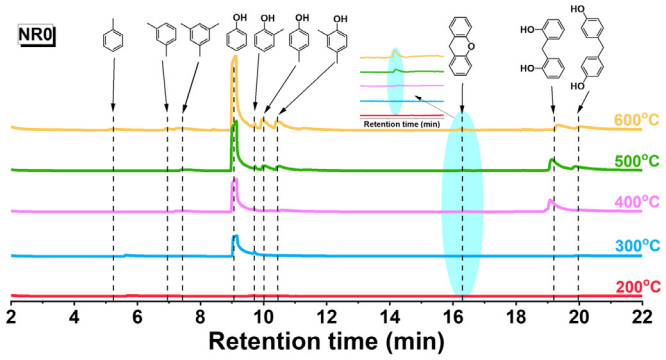

Fig. 2. The Py-GC/MS results for released pyrolysis products obtained from NR0 at different pyrolysis temperatures.

H_2O and H_2 are mainly formed through the reaction of hydrogen radicals with hydroxyl and hydrogen groups in the system, respectively. The formation of other permanent gases (such as CO, CO_2 and CH_4) is more difficult due to the need to involve the cleavage of the backbone [36,37].

The pyrolysis of the NR backbone occurs through the random cleavage of C—C single bonds, resulting in a decrease in the molecular weight of NR. Among them, the cleavage of the terminal C—C single bonds leads to the formation of monophenols or bisphenols, and their volatilization resulted in weight loss. Our previous study [38] has shown that the free monophenols or bisphenols are completely volatilized below 300 °C. The formed monophenols and bisphenols during pyrolysis can be seen in the Py-GC/MS results. In contrast, the polyphenolic compounds (such as trimers and tetramers) with higher molecular weight are difficult to volatilize and cannot be detected and show in the spectra. These involatile polyphenols further decompose to form monophenols and bisphenols VOCs with a great chance because of their short molecular link relative to NR. As shown in **Fig. 2**, the VOCs recorded by the Py-GC/MS perfectly reflect the pyrolysis process. At the pyrolysis temperature of 200 °C, few peaks corresponding to the impurities arise in the spectra. Theoretically, the free phenol in NR is also detectable by the Py-GC/MS; however, no relevant signal appears in the spectra, indicating that the free phenol content in NR0 is too low to be detected. These results are consistent with the liquid chromatography data of our previous work [38]. At the pyrolysis temperature of 300 °C, the pyrolysis products with high boiling points can be observed, such as phenol (9.32 min), *ortho*-methyl phenol (9.95 min), and 4, 4′-dihydroxydiphenylmethane (4, 4′-DHDM) (20.01 min). The NR chains undergo no significant pyrolysis at 300 °C. At the pyrolysis temperatures of 400 and 500 °C, *ortho*-methyl phenol (9.95 min) and 2, 2′-DHDM (19.32 min) are sighted in the Py-GC/MS spectra due to the CR_o process. The *para*-methyl phenol content in the pyrolysis products is higher than that of *ortho*-methyl phenol, indicating that the number of benzene

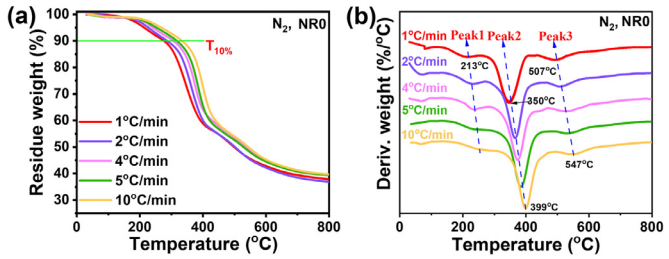

Fig. 3. The (a) TG and (b) DTG curves of NR0 under different heating rates.

rings substituted by *para* in NR0 is higher than *ortho*. At the pyrolysis temperature of 600 °C, toluene (5.19 min), xylene (6.91 min), trimethyl benzene (8.40 min), and xanthene (16.28 min) are detected in the Py-GC/MS spectra, whose origin is the violent pyrolysis of NR backbone. The deoxidization leads to the pyrolysis of aromatic rings at 600 °C. Xanthene is formed by the dehydration of hydroxyl groups in 2, 2′-DHDM [39].

Thus, according to the Py-GC/MS results, NR is stable below 300 °C and the C—C single bonds in the backbone begin to cleavage above 300 °C. A variety of radicals emerge during the cleavage process of covalent bonds. Suppose these radicals do not turn into other VOCs, they will remain in the system to further pyrolyze into other VOCs with lower molecular weight or combine with other radicals to be species with higher molecular weight. The volatilization of monophenols and bisphenols generated from the pyrolysis of terminal C—C single bonds resulted in weight loss. Although each C—C single bond in the NR backbone has the same cleavage probability, the cleavage of terminal C—C single bonds exerts a fatal impact on the char yield of NR. Therefore, decreasing the number of terminal groups in NR by increasing its molecular weight was the key to improving the char yield at high temperatures.

3.1.2. The pyrolysis process of NR

The TG analyses were used to analyze the relationship between the weight loss and the pyrolysis reaction of NR and complete the information gathered via the Py-GC/MS. It is noteworthy that, since the weight loss is only caused by the pyrolysis products volatilized at a specific temperature, the TG data cannot reflect all the pyrolysis reactions of NR. Besides, the pyrolysis products with high boiling points may further form species with a higher molecular weight that cannot lead to the corresponding TG-detected weight loss. From this perspective, the quantitative kinetic analysis by the TG is somewhat far-fetched. The free bisphenols in NR0 can volatilize at temperatures far below their boiling points of 360 - 390 °C. This process occurred before the cleavage of NR, as evidenced by the weight loss below 300 °C in the relevant TG curves (referred to as Peak 1 in **Fig. 3** (b)). The influence of free bisphenols on the weight loss processes of NR was demonstrated in Ref. [38].

In **Fig. 3** (b), the emergence of Peak 2 verifies the volatilization of pyrolysis products, which are resulted from the cleavage reactions of the covalent single bonds in the NR molecular. The slight differences in the cleavage order of the various covalent single bonds resulted from their stability [40,41], which can be reflected by molecular dynamics simulation [31], whereas the TG analysis cannot clearly distinguish the cleavage order of these covalent single bonds. Many radicals are formed through the cleavage of the covalent single bonds, resulting in the rapid formation of H_2O, permanent gases, and phenolic VOCs. The escape of VOCs resulted in the second weight loss peak observed from the TG curves (Peak 2 in **Fig. 3** (b)), and this weight loss process corresponded to the second weight loss of the cured PR reported in the literature [42]. Although the number of VOCs is small compared with H_2O, they generally cause a relatively significant weight loss due to the high relative molecular mass. In other words, the volatilization of H_2O and H_2 mainly affects the thermal decomposition temperature of NR, but does not determine the char yield. On the contrary, the release of VOCs formed by the CR_o process exerts influence on both the thermal decomposition temperature and char yield of NR. Finally, the weight loss between 500 °C and 600 °C in the TG curves (Peak 3 in **Fig. 3** (b)) corresponded to the benzene dehydrogenation processes [43].

On the other hand, the thermal decomposition temperature and char yield of NR are strongly dependent on the heating rates in TG tests. At relatively high heating rates, the pyrolysis reactions are not completed within the relevant temperature range, leading to increased thermal decomposition temperature. In turn, the lower heating rates provide enough time to complete pyrolysis reactions, being beneficial to observing the pyrolysis process. For example, the $T_{10\%}$ values of NR0 at heating rates of 1 °C/min and 10 °C/min are 286.1 °C and 334.0 °C, respectively (**Table S6**). In addition, the thermal decomposition temperature of NR is lower than PE or PP composed of carbon skeleton [44]. The bond dissociation energy of C—C and C—H single bonds are not so low as to decrease the thermal decomposition temperature of NR. Therefore, one can infer that the lower thermal decomposition temperature of NR is caused by reducing the covalent bond stability [41] due to the aromatic ring structure and the volatilization of free monophenols and bisphenols.

3.2. The influence of molecular weight and crosslinking on the pyrolysis process of NR

According to the above results, the intense weight loss of NR0 between 300 and 500 °C results from the cleavage of the covalent single bonds. Significantly, the release of free monophenols and bisphenols formed by the cleavage of C—C single bonds close to the end of the molecule had a fatal effect on the char yield of NR0. NR is featured by the polydispersity, at which the NR chains with higher molecular weights are less likely to form VOCs due to the lower terminal group content. To study the effect of molecular weight on the pyrolysis process of NR, we have prepared five fractions with different molecular weights by phase separation of NR0 (**Figure S1 - 3, Table S2**), and the fractions with decreasing molecular weight are named NR1, NR2, NR3, NR4, and NR5. As seen in **Fig. 4** (c), the weight loss of NR above 300 °C gradually decreased with increasing molecular weight. The results show that the char yield of NR gradually increases as the amounts of monophenols and bisphenols formed by the CR_o process decreases. However, as the molecular weight of NR increases, the effect of molecular weight on the char yield gradually weakens.

Furthermore, the crosslinking of NR can also reduce the content of terminal groups and improve the char yield of NR. The introduction of HMTA into NR increases the crosslinking degree and eliminates a part of the terminal groups, thus improving the char yield of NR (**Fig. 4** (c)). However, the existence of terminal groups is inevitable due to the limited crosslinking degree and the new terminal group will be formed due to the cleavage of C—C single bonds, inducing the release of VOCs during the pyrolysis process of cured HNR. The possibility of VOCs formation decreases with the increasing crosslinking degree of HNR, which is conducive to the char yield. However, as the crosslinking degree increases, the effect on the char yield gradually weakens, and once the cured HNR reaches the saturated crosslinking degree, its char yield will decrease. For example, the char yield of the HNR-16 was 62.0%, inferior to that of the HNR-12 (63.0%). The main reason is the rigid skeleton of NR [45] and the limited number of reactive sites on phenol, which determines that the crosslinking density of HNR will reach saturation as the dosage of HMTA increases. For NR0 with a number average molecular weight of 908, when the

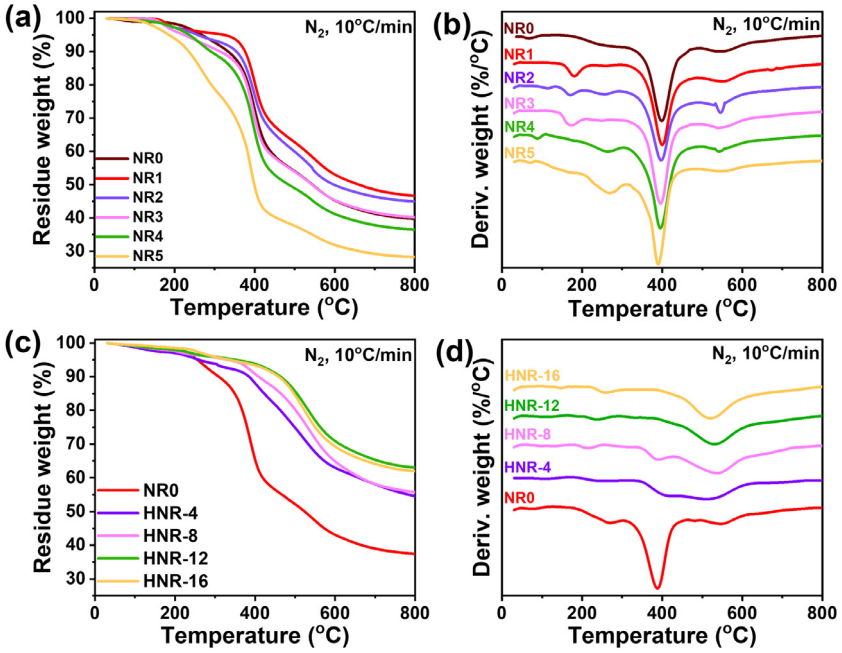

Fig. 4. The (a) TG and (b) DTG curves of NR0 and its various fractions, the (c) TG and (d) DTG curves of NR0 cured by HMTA.

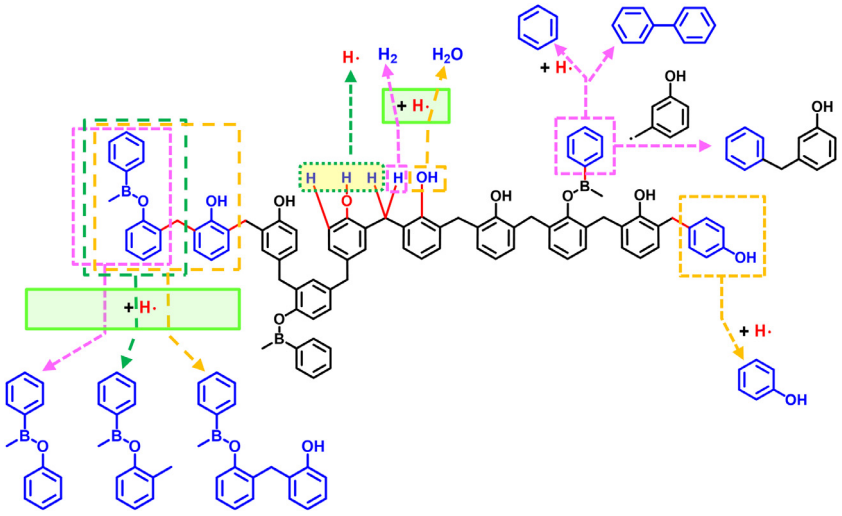

Scheme 2. The pyrolysis process of PBNR.

dosage of HMTA is 12 phr the molar ratio of methylene groups in HMTA to that of phenols in NR0 is about 0.5, which means that the methylene groups are wholly consumed theoretically by the phenol. When the dosage of HMTA increased from 12 phr to 16 phr, the nitrogen-containing structure in the crosslinking network increased [32]. These nitrogen-containing structures contribute little to the crosslinking density of HNR and will cause weight loss during the pyrolysis process [46], reducing the char yield of HNR.

3.3. The pyrolysis mechanism of PBNR

3.3.1. The homolytic reaction and the formation of VOCs during PBNR pyrolysis

Our previous studies [25,34] revealed the curing reaction between boron hydroxyl groups and phenol hydroxyl groups during the curing of PBNR, which led to the formation of the crosslinking structure featured by the boronic ester linkages. The presence of boronic ester linkages increases the molecular weight of generated small molecular compounds and makes them difficult to become VOCs. Furthermore, the boronic ester linkages change the pyrolysis process of NR to retain VOCs from the terminal group cleavage (**Scheme 2**).

The Py-GC/MS analyses show that both the types and quantities of pyrolysis products for PBNR and NR at high temperatures are significantly different, which can be reflected in the following two aspects. On the on hand, the monophenols and bisphenol contents in the pyrolysis products of PBNR decrease considerably due to the formation of many boronic ester linkages. The crosslinking by boronic ester linkages increased the molecular weight of VOCs formed by the CR_o process, thus preventing their release and then improving the char yield relative to NR. The quantitative information of PBNR products at different pyrolytic temperatures (**Table S3**) could be obtained from Py-GC/MS (**Fig. 5**). The relative content of each pyrolytic product could be expressed as the percentage of the peak area. We calculated the relative content of monophenols (Peak 2#, Peak 3#, Peak 4#, and Peak 5#) and bisphenols (Peak 13#, Peak 14#, Peak 15#, Peak 16#, and Peak 17#). As shown in **Fig. 6** (a), the relative contents of monophenols and bisphenols decrease

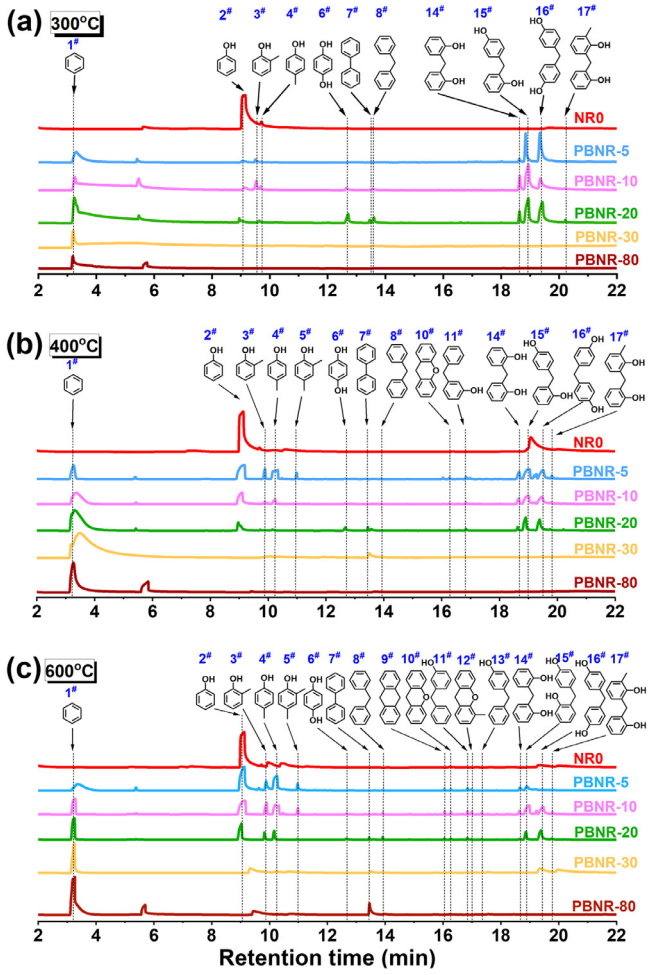

Fig. 5. The Py-GC/MS results for released pyrolysis products of PBNR at different pyrolysis temperatures: (a) 300 °C; (b) 400 °C; (c) 600 °C.

with the increase of PBA. For example, the relative contents of monophenols and bisphenols in the pyrolytic products of PBNR-30 at 400 °C are respectively 3.5% and 0, which is significantly lower than these of NR0 (65.6% and 34.4%). Therefore, the formation of boronic ester linkages significantly inhibits the monophenols and bisphenols VOCs generated during the NR pyrolysis process, and this inhibitory effect increases with the increasing dosage of PBA.

On the other hand, the comparative analysis of the Py-GC/MS data of NR with PBNR enables one to conclude that benzene and biphenyl are the pyrolysis products of PBNR resulted from the cleavage of B—C bonds. The benzene radicals can react with the hydrogen radical to form benzenes and benzene radicals to be biphenyls (**Scheme 2**). We analyzed the relative content of benzene (Peak 1#) and biphenyl (Peak 6#) in the pyrolytic products of PBNR-30 (**Fig. 6** (b)). The benzene content in the NR pyrolytic products is almost 0, while the relative contents of benzene in the PBNR-5 and PBNR-30 pyrolytic products are 14.32% and 93.65%, respectively. In particular, the appearance of biphenyl at 600 °C indicates that benzene radicals have increased significantly. The relative contents of biphenyl in the pyrolytic products of PBNR-30 and PBNR-80 are 2.61% and 9.47%. Therefore, the effect of PBA on the pyrolysis process of NR is reflected in two aspects. On the one hand, the formation of boronic ester linkages inhibits the generation of phenolic VOCs; on the other hand, the cleavage of the B—C bond produces benzene VOCs.

3.3.2. *The pyrolysis process of PBNR*

The high reaction temperature between boron hydroxyl groups and phenol hydroxyl groups and the dynamic reversibility of boronic ester linkages make it difficult to convert boron hydroxyl groups into boronic ester linkages [47–49]. As a result, some boron hydroxyl groups and phenol hydroxyl groups remain in the system even after the prolonged curing time. The boron hydroxyl group reacts with the phenolic hydroxyl group or the boron hydroxyl group to form boronic ester / boroxane linkages and produce water, leading to the obvious weight loss at a low temperature (ca. 214 °C), as seen in the corresponding TG curves **Fig. 7** (a). Therefore, the thermal decomposition temperature of PBNR is lower than that of NR.

The turning point of the TG curves for NR and PBNR appears near 350 °C (**Fig. 7** (a)). A large number of C—C single bonds are broken near this temperature, resulting in the significant weight loss of NR. However, the formed boronic ester linkages play important roles at the moment. As shown in **Fig. 5** (a), NR begins to pyrolyze at about 300 °C, leading to the release of numerous phenolic VOCs (such as monophenols and bisphenols). For PBNR, the VOCs formed by the CR_o process are "locked" and retains in the system by the boronic ester linkages, so the weight loss of PBNR above 300 °C tends to decrease with the increase of PBA dosage. It is noteworthy that the cleavage of B—C bonds in PBNR at about 300 °C causes the temperature of the maximum degradation rate (T_{max}) of PBNR to be higher than that of NR. For example, the T_{max} of PBNR-10 and PBNR-30 are about 373 °C and 328 °C, respectively. The boronic ester linkages partially block the phenol hydroxyl groups and improve the thermal stability of the NR backbone, leading to the higher T_{max} of PBNR (about 500 °C). It thereby appears that inhibiting the release of VOCs greatly contributes to

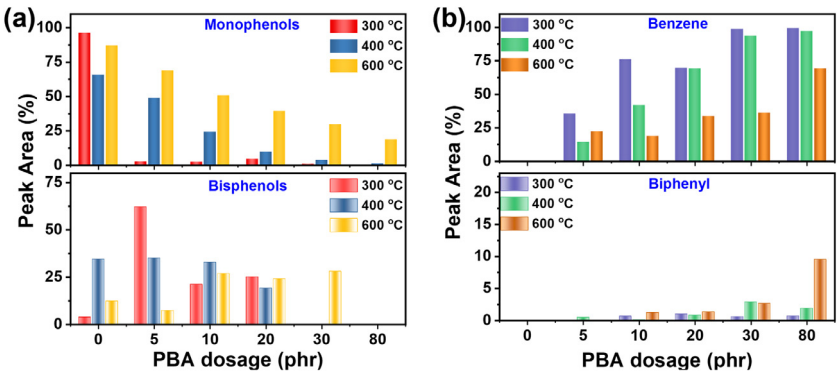

Fig. 6. VOCs released during pyrolysis process of PBNR based on Py-GC/MS analyses. (a) is the effect of PBA dosage on the amount of monophenol and bisphenol; (b) is the effect of PBA dosage on the amount of benzene and biphenyl.

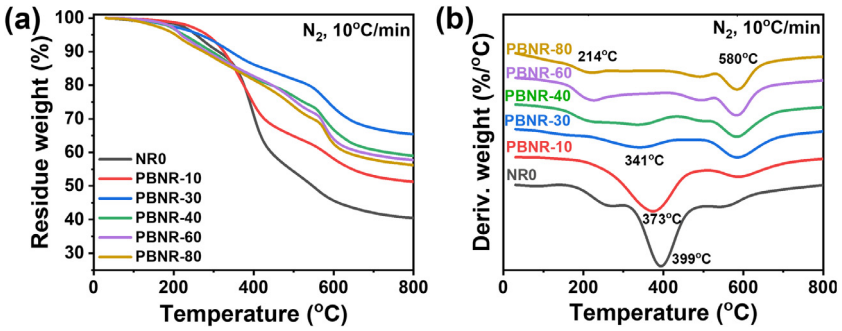

Fig. 7. (a) TG and (b) DTG curves of PBNR with various PBA dosages.

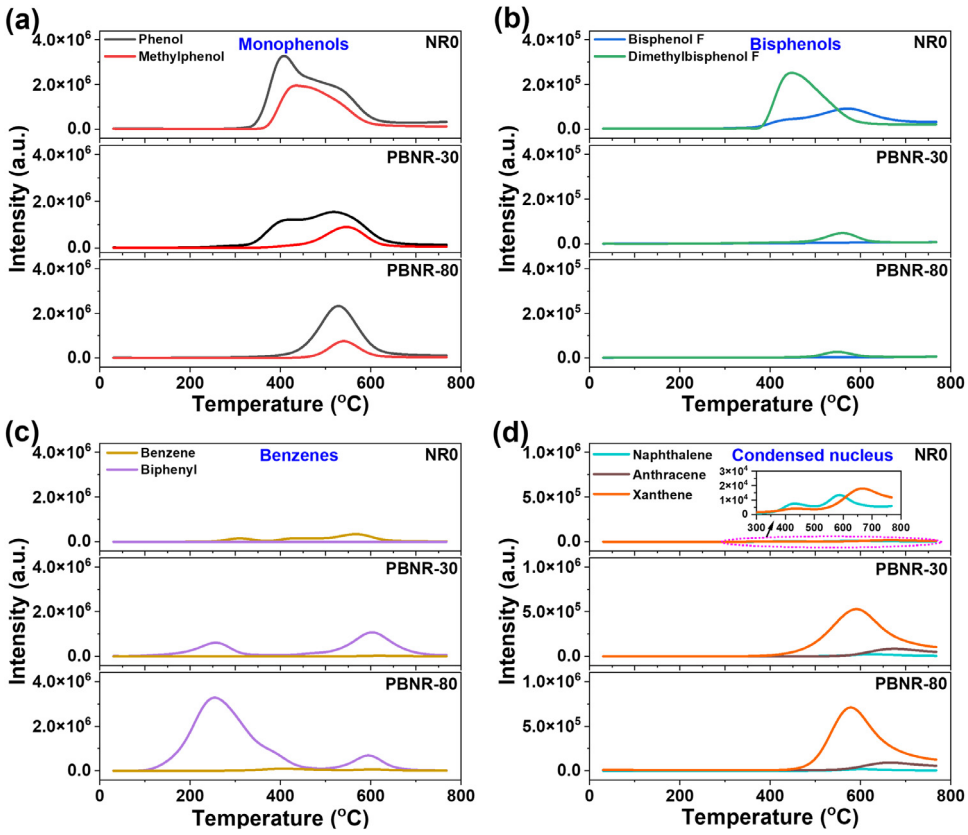

Fig. 8. (a), (b), (c) and (d) are the changes in the number of the monophenols, bisphenols, benzenes and fused-ring aromatic hydrocarbons with temperature. In order to facilitate the comparison of the results of different PBA dosages, the ordinates of the figure are set to the same range. The heating rate of TGA is 10 °C/min.

the char yield of PBNR. A noticeable increase in the weight loss of PBNR was observed close to 600 °C, due to the formation of fused-ring aromatic hydrocarbons (Fig. 8 (d)).

With the increasing PBA dosage, the char yield of PBNR first increases and then decreases. The B—C bonds start to pyrolyze at above 100 °C, resulting in the stripping of benzene rings and the weight loss of PBNR. For the PBNR with the high PBA dosage (more than 30 phr), the contribution of PBA to the crosslinking of the system is offset by the volatilization of the benzene rings resulting from the cleavage of B—C bonds. The effect of the volatilization of benzene on the weight loss of PBNR is mainly reflected in the reduction of the thermal decomposition temperature and char yield. As shown in Table 1, the $T_{10\%}$ decreased with the increasing PBA dosage. The main reason is the $T_{10\%}$ is in the temperature range where many B—C bonds are broken. However, the volatilization of benzene cannot wholly offset the inhibitory effect of the boronic ester linkages on the volatilization of phenolic VOCs, and the char yield of PBNR is still much higher than that of NR. For example, the $R_{800°C}$ of PBNR-30 is 59.2%, which is much higher than 40.5% of NR0. On the other hand, the condensation reaction of PBAs, resulting in the B—O—B structure (such as boroxine) [46] in the cured PBNR with excessive PBA dosage, leads to the formation of

Table 1
TGA data of the PBNR with different dosages of PBA.

Resin	$T_{10\%}$ [a] (°C)	T_{max} [b] (°C)	$R_{800°C}$ [c] (%)
NR0	312.0	398.7	40.5
PBNR-10	325.5	379.2	51.3
PBNR-30	303.0	585.0	59.2
PBNR-40	295.7	583.5	59.0
PBNR-60	282.8	582.8	57.7
PBNR-80	274.5	584.3	56.2

[a] Thermal decomposition temperature at 10% weight loss.
[b] Maximum rate of the weight loss.
[c] Residue weight at 800 °C.

invalid linkages for crosslinking. Compared with the B—O—C linkages, these B—O—B linkages contribute less to the crosslinking of PBNR, especially NR cannot be crosslinked when PBA is condensed to form a boroxine structure.

The TGA-GC/MS-FTIR technology was used to analyze the pyrolysis process of NR0, PBNR-30, and PBNR-80 (**Figs. 8** and **9**) to clarify further the influence of the boronic ester linkages on the pyrolysis mechanism. The weight loss of NR during its pyrolysis is mainly caused by the volatilization of monophenols and bisphenols VOCs. It can be seen from **Fig. 8** (a) and (b) that the boronic ester linkages significantly reduce the number of monophenols and bisphenols. However, the benzenes VOCs of PBNR-30 and PBNR-80 can be generated above 100 °C (**Fig. 8** (c)), and the amount of benzenes VOCs increases significantly with the increase of the dosage of PBA, which is the main reason why the decomposition temperature and char yield of PBNR-80 are lower than these of PBNR-30. The TGA-FTIR spectra (**Fig. 9**) can further confirm the conclusions obtained by TGA-GC/MS. The features observed at 3500–3800 cm^{-1} and 1258 cm^{-1} are attributed to the O—H and C—O stretching modes of phenol, and 670 cm^{-1} is attributed to the C—H of benzene. The signals of phenolic products in PBNR are weakened, while the signals of benzene products are enhanced.

3.3.3. *Temperature-induced pyrolysis reaction of PBNR*

As mentioned above, the temperature ranges for the intense weight loss of PBNR are 300 to 400 °C and 500 to 600 °C. We assume that the pyrolysis of PBNR is temperature-induced, meaning that there is a kinetically dominant pyrolysis process at each temperature scale. To confirm this conjecture, the PBNR-30 was heated with different heating rates and heated rapidly to a specific temperature at the heating rate of 100 °C/min and then kept for 2 h (**Fig. 10**). The results showed that no new pyrolysis reactions are activated at the specific temperature by prolonging the time, and those of PBNR are therefore temperature-induced. This conclusion lays the foundation for discussing the pyrolysis process of NR according to temperature ranges and provides the basis for understanding the thermal stability of PR.

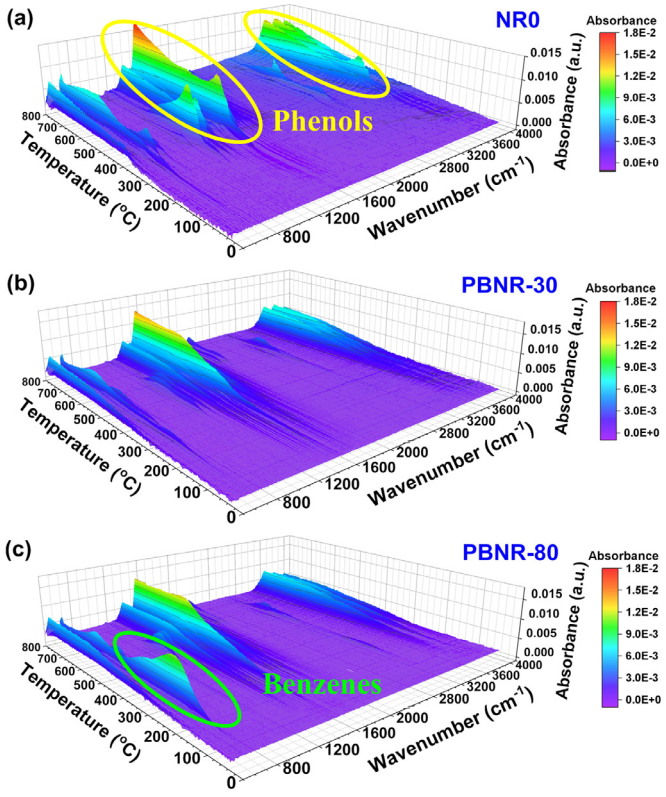

Fig. 9. The TGA-FTIR spectra of (a) NR0, (b) PBNR-30 and (c) PBNR-80. The heating rate of TGA is 10 °C/min, and the resolution of FTIR is 8 cm^{-1}.

The weight loss value of PBNR in the process of 2 h at different temperatures can also reflect the intensity of the pyrolysis reaction of the sample. We have calculated the weight loss of PBNR at different temperatures for 2 h (**Fig. 10** (d), **Table S7**). The curve of weight loss and temperature is similar to the DTG curve with a heating rate of 100 °C/min. There are two significant weight loss

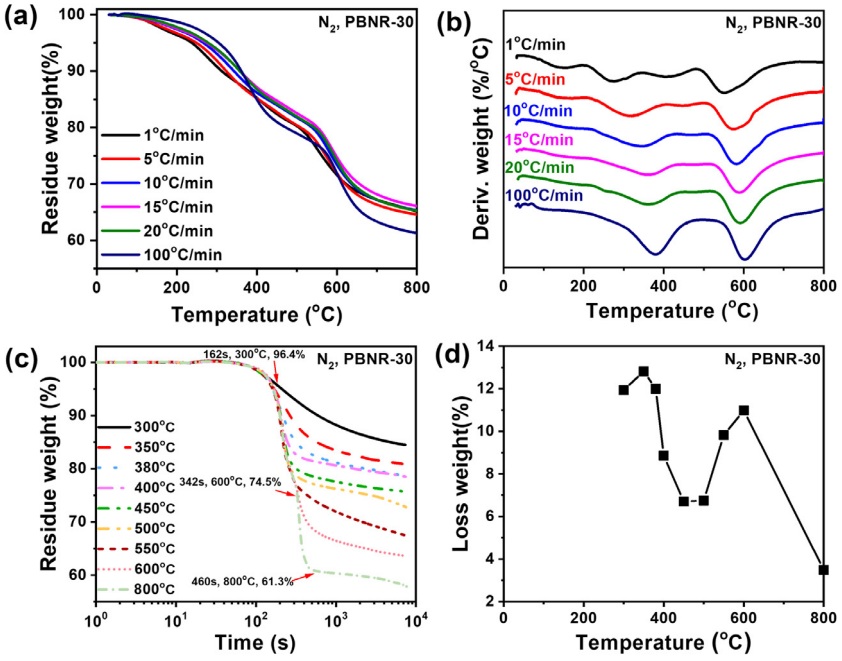

Fig. 10. The TG results of PBNR-30. The (a) TG and (b) DTG curves of PBNR-30 at different heating rates; (c) The TG curves of PBNR-30 at constant temperature (nitrogen protection, heated up to the required temperature at the heating rate of 100 °C/min, and then kept for 2 h); (d) The loss weight of PBNR-30 at constant temperatures.

values at 350 °C and 600 °C, which are basically consistent with the peak temperatures (341 °C and 585 °C) of weight loss peaks in the DTG curve that can reflect the thermal weight loss rate.

4. Conclusions

In conclusion, this study fundamentally illustrated the reason for the weight loss of NR and PBNR during the pyrolysis process at high temperatures. The pyrolysis of NR originated from the cleavage reaction of covalent single bonds, and these reactions were divided into the CR_o and CR_b. The release of phenolic VOCs formed during the CR_b process resulted in the weight loss of NR. The increasing molecular weight and the crosslinking of NR were beneficial to reducing phenolic VOCs, thereby increasing the char yield of NR. The formation of the boronic ester linkages in PBNR changed the pyrolysis mechanism of NR, improving the thermal stability of cured resin at high temperatures, and reducing the volatilization possibility of phenolic VOCs during the pyrolysis process. The higher PBA dosage increased the probability of the cleavage of B—C bonds during the pyrolysis, leading to the stripping of benzene. The char yield of PBNR first increased with increasing PBA until the PBA dosage reached 30 phr. The pyrolysis reaction of PBNR was temperature-induced, meaning that prolonging the reaction time at low temperatures will not trigger the pyrolysis reactions that occur at higher temperatures. This study revised the previous understanding of the high char yield of PBPR, and provided theoretical guidance to reduce the weight loss in essence, which is of great advantage to improve the thermal stability of PR and broaden the application of PR in the field of ablation-resistant composite materials.

Declaration of Competing Interest

The authors declare that they have no known competing financial interests or personal relationships that could have appeared to influence the work reported in this paper.

CRediT authorship contribution statement

Xiaolong Xing: Methodology, Investigation, Formal analysis, Visualization, Writing – original draft. **Ping Zhang:** Methodology, Investigation, Validation, Data curation, Writing – original draft. **Yuhong Zhao:** Writing – review & editing. **Fei Ma:** Supervision, Funding acquisition. **Xiaoting Zhang:** Writing – review & editing. **Fang Xue:** Supervision, Funding acquisition. **Shujuan Wang:** Writing – review & editing. **Xinli Jing:** Conceptualization, Supervision, Project administration, Writing – original draft, Writing – review & editing, Resources, Funding acquisition.

Acknowledgments

This work is supported by the National Natural Science Foundation of China (No. 51273160, 51473134, 51703179), National Key Research and Development Program of China (No. 2019YFA0706801), and Fundamental Research Funds for the Central Universities (No. xjh012019024). We also acknowledge the Instrument Analysis Centre of Xi'an Jiaotong University for material characterization.

Supplementary materials

Supplementary material associated with this article can be found, in the online version, at doi:10.1016/j.polymdegradstab.2021.109672.

References

[1] D. Crespy, M. Bozonnet, M. Meier, 100 years of bakelite, the material of a 1000 uses, Angew. Chem. Int. Ed. Engl. 47 (18) (2008) 3322–3328, doi:10.1002/anie.200704281.
[2] A.P. Singh, P. Garg, F. Alam, K. Singh, R.B. Mathur, R.P. Tandon, A. Chandra, S.K. Dhawan, Phenolic resin-based composite sheets filled with mixtures of reduced graphene oxide, gamma-Fe_2O_3 and carbon fibers for excellent electromagnetic interference shielding in the X-band, Carbon 50 (10) (2012) 3868–3875, doi:10.1016/j.carbon.2012.04.030.
[3] H.Y. Jiang, J.G. Wang, S.Q. Wu, Z.Q. Yuan, Z.L. Hu, R.M. Wu, Q.L. Liu, The pyrolysis mechanism of phenol formaldehyde resin, Polym. Degrad. Stab. 97 (8) (2012) 1527–1533, doi:10.1016/j.polymdegradstab.2012.04.016.
[4] J.G. Wang, H.Y. Jiang, N. Jiang, Study on the pyrolysis of phenol-formaldehyde (PF) resin and modified PF resin, Thermochim. Acta 496 (1-2) (2009) 136–142, doi:10.1016/j.tca.2009.07.012.
[5] H.M. Cheng, H.F. Xue, C.Q. Hong, X.H. Zhang, Preparation, mechanical, thermal and ablative properties of lightweight needled carbon fibre felt/phenolic resin aerogel composite with a bird's nest structure, Compos. Sci. Technol. 140 (2017) 63–72, doi:10.1016/j.compscitech.2016.12.031.
[6] K. Ouchi, Infra-red study of structural changes during pyrolysis of a phenol-formaldehyde resin, Carbon 4 (1) (1966) 59–66, doi:10.1016/0008-6223(66)90009-1.
[7] W.M. Jackson, R.T. Conley, High temperature oxidative degradation of phenol–formaldehyde polycondensates, J. Appl. Polym. Sci. 8 (5) (1964) 2163–2193, doi:10.1002/app.1964.070080516.
[8] J.G. Gao, Y.F. Liu, L.T. Yang, Thermal stability of boron-containing phenol formaldehyde resin, Polym. Degrad. Stab. 63 (1) (1999) 19–22, doi:10.1016/S0141-3910(98)00056-1.
[9] J.G. Gao, Y.F. Liu, F.L. Wang, Structure and properties of boron-containing bisphenol-A formaldehyde resin, Eur. Polym. J. 37 (1) (2001) 207–210, doi:10.1016/S0014-3057(00)00095-1.
[10] S. Li, F.H. Chen, B.X. Zhang, Z.H. Luo, H. Li, T. Zhao, Structure and improved thermal stability of phenolic resin containing silicon and boron elements, Polym. Degrad. Stab. 133 (2016) 321–329, doi:10.1016/j.polymdegradstab.2016.07.020.
[11] L.M. Kindley, N. Filipescu, E. Pappas, C. Heuther, Phosphorus-containing phenolic resins, SPE Trans. 4 (2) (1964) 139–143, doi:10.1002/pen.760040216.
[12] Y. Horie, S. Shiraishi, A. Oya, Preferential supporting of platinum particles on pore surface using a polymer blend technique, J. Mater. Sci. Lett. 20 (2) (2001) 105–106, doi:10.1023/A:1006721830541.
[13] S. Li, F.H. Chen, Y. Han, H. Zhou, H. Li, T. Zhao, Enhanced compatibility and morphology evolution of the hybrids involving phenolic resin and silicone intermediate, Mater. Chem. Phys. 165 (2015) 25–33, doi:10.1016/j.matchemphys.2015.07.054.
[14] S. Li, Y. Han, F.H. Chen, Z.H. Luo, H. Li, T. Zhao, The effect of structure on thermal stability and anti-oxidation mechanism of silicone modified phenolic resin, Polym. Degrad. Stab. 124 (2016) 68–76, doi:10.1016/j.polymdegradstab.2015.12.010.
[15] S. Li, H. Li, Z. Li, H. Zhou, Y. Guo, F.H. Chen, T. Zhao, Polysiloxane modified phenolic resin with co-continuous structure, Polymer 120 (2017) 217–222, doi:10.1016/j.polymer.2017.05.063.
[16] W.F. Zhang, C.L. Liu, Y.G. Ying, W.S. Dong, The preparation and characterization of boron-containing phenolic fibers, Mater. Chem. Phys. 121 (1–2) (2010) 89–94, doi:10.1016/j.matchemphys.2009.12.042.
[17] A.P. Sporzynski, S.B. Twiss, Resinous Material from a Phenyl Borate and an Aldehyde, 1951 US.
[18] J.G. Gao, C.J. Jiang, X.H. Su, Synthesis and thermal properties of boron-nitrogen containing phenol formaldehyde resin/MMT nanocomposites, Int. J. Polym. Mater. 59 (8) (2010) 544–552, doi:10.1080/00914031003760659.
[19] M.O. Abdalla, A. Ludwick, T. Mitchell, Boron-modified phenolic resins for high performance applications, Polymer 44 (24) (2003) 7353–7359, doi:10.1016/j.polymer.2003.09.019.
[20] C. Martin, J.C. Ronda, V. Cadiz, Boron-containing novolac resins as flame retardant materials, Polym. Degrad. Stab. 91 (4) (2006) 747–754, doi:10.1016/j.polymdegradstab.2005.05.025.
[21] Y.H. Liu, X.L. Jing, Pyrolysis and structure of hyperbranched polyborate modified phenolic resins, Carbon 45 (10) (2007) 1965–1971, doi:10.1016/j.carbon.2007.06.008.
[22] P.J. Xu, X.L. Jing, Pyrolysis of hyperbranched polyborate modified phenolic resin, Polym. Eng. Sci. 50 (7) (2010) 1382–1388, doi:10.1002/pen.21675.
[23] J.J. Si, P.J. Xu, W. He, S.J. Wang, X.L. Jing, Bis-benzoxazine resins with high char yield and toughness modified by hyperbranched poly(resorcinol borate), Compos Part A-Appl S 43 (12) (2012) 2249–2255, doi:10.1016/j.compositesa.2012.07.025.
[24] S.J. Wang, X.L. Jing, Y. Wang, J.J. Si, Synthesis and characterization of phenolic resins containing aryl-boron backbone and their utilization in polymeric composites with improved thermal and mechanical properties, Polym. Advan. Technol. 25 (2) (2014) 152–159, doi:10.1002/pat.3216.
[25] S.J. Wang, X.L. Jing, Y. Wang, J.J. Si, High char yield of aryl boron-containing phenolic resins: the effect of phenylboronic acid on the thermal stability and carbonization of phenolic resins, Polym. Degrad. Stab. 99 (2014) 1–11, doi:10.1016/j.polymdegradstab.2013.12.011.
[26] N. Kizilcan, P. Dincer, In situ modification of cyclohexanone formaldehyde resin with boric acid for high-performance applications, J. Appl. Polym. Sci. 129 (5) (2013) 2813–2820, doi:10.1002/app.38951.

[27] C. Cheng, X.G. Zhang, Y.X. Wang, L. Sun, C.X. Li, Phenylboronic acid-containing block copolymers: synthesis, self-assembly, and application for intracellular delivery of proteins, New J. Chem. 36 (6) (2012) 1413–1421, doi:10.1039/c2nj20997g.
[28] S.J. Wang, Y. Wang, C. Bian, Y.H. Zhong, X.L. Jing, The thermal stability and pyrolysis mechanism of boron-containing phenolic resins: the effect of phenyl borates on the char formation, Appl. Surf. Sci. 331 (2015) 519–529, doi:10.1016/j.apsusc.2015.01.062.
[29] S. Balci, N.A. Sezgi, E. Eren, Boron oxide production kinetics using boric acid as raw material, Ind. Eng. Chem. Res 51 (34) (2012) 11091–11096, doi:10.1021/ie300685x.
[30] Q. Lu, F. Chen, Q. Shen, Y. Qin, Z.X. Huang, L.M. Zhang, Pyrolysis behavior of boron-containing phenol-formaldehyde resin (BPFR) modified by B_2O_3, Adv. Ceram. Novel Process. 616 (2014) 315–318, doi:10.4028/www.scientific.net/KEM.616.315.
[31] X. Xing, X. Niu, Y. Liu, C. Yang, S. Wang, Y. Li, X. Jing, In-depth understanding on the early stage of phenolic resin thermal pyrolysis through ReaxFF-molecular dynamics simulation, Polym. Degrad. Stab. 186 (2021) 109534, doi:10.1016/j.polymdegradstab.2021.109534.
[32] Y. Wang, S.J. Wang, C. Bian, Y.H. Zhong, X.L. Jing, Effect of chemical structure and cross-link density on the heat resistance of phenolic resin, Polym. Degrad. Stab. 111 (2015) 239–246, doi:10.1016/j.polymdegradstab.2014.11.016.
[33] J. Monni, P. Niemela, L. Alvila, T.T. Pakkanen, Online monitoring of synthesis and curing of phenol-formaldehyde resol resins by Raman spectroscopy, Polymer 49 (18) (2008) 3865–3874, doi:10.1016/j.polymer.2008.06.050.
[34] S.J. Wang, X.L. Xing, X.T. Zhang, X. Wang, X.L. Jing, Room-temperature fully recyclable carbon fibre reinforced phenolic composites through dynamic covalent boronic ester bonds, J. Mater. Chem. A 6 (23) (2018) 10868–10878, doi:10.1039/c8ta01801d.
[35] B. Singh, N. Sharma, Mechanistic implications of plastic degradation, Polym. Degrad. Stab. 93 (3) (2008) 561–584, doi:10.1016/j.polymdegradstab.2007.11.008.
[36] Y.H. Zhong, X.L. Jing, S.J. Wang, Q.X. Jia, Behavior investigation of phenolic hydroxyl groups during the pyrolysis of cured phenolic resin via molecular dynamics simulation, Polym. Degrad. Stab. 125 (2016) 97–104, doi:10.1016/j.polymdegradstab.2015.11.017.
[37] K.A. Trick, T.E. Saliba, Mechanisms of the pyrolysis of phenolic resin in a carbon/phenolic composite, Carbon 33 (11) (1995) 1509–1515, doi:10.1016/0008-6223(95)00092-R.
[38] P. Zhang, S.J. Wang, X.T. Zhang, X.L. Jing, The effect of free dihydroxydiphenylmethanes on the thermal stability of novolac resin, Polym. Degrad. Stab. 168 (2019) 108946, doi:10.1016/j.polymdegradstab.2019.108946.
[39] M.L.N. Rao, B.S. Ramakrishna, Rh-catalyzed direct synthesis of 2,2′-dihydroxybenzophenones and xanthones, RSC Adv 6 (79) (2016) 75505–75511, doi:10.1039/c6ra18647e.
[40] C. Bian, Y. Wang, S.J. Wang, Y.H. Zhong, Y. Liu, X.L. Jing, Influence of borate structure on the thermal stability of boron-containing phenolic resins: a DFT study, Polym. Degrad. Stab. 119 (2015) 190–197, doi:10.1016/j.polymdegradstab.2015.05.009.
[41] C. Bian, S.J. Wang, Y.H. Liu, X.L. Jing, Thermal stability of phenolic resin: new insights based on bond dissociation energy and reactivity of functional groups, RSC Adv. 6 (60) (2016) 55007–55016, doi:10.1039/c6ra07597e.
[42] Y.F. Chen, Z.Q. Chen, S.Y. Xiao, H.B. Liu, A novel thermal degradation mechanism of phenol-formaldehyde type resins, Thermochim. Acta 476 (1–2) (2008) 39–43, doi:10.1016/j.tca.2008.04.013.
[43] E. Fitzer, W. Schafer, Effect of crosslinking on formation of glasslike carbons from thermosetting resins, Carbon 8 (3) (1970) 353–364, doi:10.1016/0008-6223(70)90075-8.
[44] P. Das, P. Tiwari, The effect of slow pyrolysis on the conversion of packaging waste plastics (PE and PP) into fuel, Waste Manage. 79 (2018) 615–624, doi:10.1016/j.wasman.2018.08.021.
[45] N.J.L. Megson, Molecular structure and its influence on the properties of phenolic resins, J. Soc. Chem. Ind.-L 67 (4) (1948) 155–160, doi:10.1002/jctb.5000670409.
[46] J. Yun, L. Chen, X. Zhang, J. Feng, L. Liu, The effect of introducing B and N on pyrolysis process of high ortho novolac resin, Polymers (Basel) 8 (3) (2016) 35, doi:10.3390/polym8030035.
[47] R. Nishiyabu, Y. Kubo, T.D. James, J.S. Fossey, Boronic acid building blocks: tools for sensing and separation, Chem. Commun. (Camb) 47 (4) (2011) 1106–1123, doi:10.1039/c0cc02920c.
[48] G. Vancoillie, R. Hoogenboom, Synthesis and polymerization of boronic acid containing monomers, Polym. Chem. 7 (35) (2016) 5484–5495, doi:10.1039/c6py00775a.
[49] W.L. Brooks, B.S. Sumerlin, Synthesis and applications of boronic acid-containing polymers: from materials to medicine, Chem. Rev. 116 (3) (2016) 1375–1397, doi:10.1021/acs.chemrev.5b00300.